J Shanghai Univ (Engl Ed), 2011, 15(6): 562–567
Digital Object Identifier(DOI): 10.1007/s11741-011-0787-2

Direct driven wind energy conversion system based on hybrid excitation synchronous machine

YE Bin-ying (叶斌英)[1], RUAN Yi (阮 毅)[1], YANG Yong (杨 勇)[2], ZHAO Mei-hua (赵梅花)[1], TANG Yan-yan (汤燕燕)[1]
1. School of Mechatronics Engineering and Automation, Shanghai University, Shanghai 200072, P. R. China
2. School of Urban Railway Transportation, Soochow University, Suzhou 215021, Jiangsu, P. R. China

Abstract A novel direct-drive type wind power generation system based on hybrid excitation synchronous machine (HESM) is introduced in this paper. The generator is connected to an uncontrollable rectifier, and a fully controlled voltage-source inverter is used to connect the system to utility grid. An intermediate DC bus exists between the rectifier and inverter. A new control strategy is proposed which achieves the maximum power point tracking (MPPT) with the control of excitation current of HESM and stabilizes the DC link voltage with the control of inverter output current simultaneously. Specially-designed buck circuit is used to control the excitation current of HESM, and grid voltage-oriented vector control strategy is employed to realize the decoupling of the inverter output power. Simulation results and experiment in 3 kW lab prototype show an excellent static and dynamic performance of the proposed system.

Keywords maximum power point tracking (MPPT), wind energy conversion system, direct-driven, hybrid excitation

Introduction

Wind power, even though abundant, varies continually as wind speed changes throughout the day[1−2]. The power of a wind turbine can absorb at a given wind velocity depending upon the angular velocity of the turbine, while there exists an optimum value. Only the capturing maximum possible power constantly from the available wind power is of utmost importance for a wind power generation system, can we make efficient use of equipment and available energy source. Therefore, both energy conversion and maximum power point tracking (MPPT) control strategy are active research area[3−16].

The typical wind conversion system technology includes fixed-speed constant-frequency and variable-speed constant-frequency types. In recent years, fixed speed wind energy conversion systems, due to poor energy capture ability in mechanical component and poor power quality, have given way to variable speed systems, which have reduced mechanical stress and aerodynamic noise, and can be controlled in order to enable the turbine operate at a maximum efficiency point in a wide range of wind velocities, capturing larger wind power than the traditional one[3−4].

There are mainly two structures of variable speed systems: One uses doubly fed induction generator (DFIG), and the other uses direct driven permanent magnet synchronous generator (PMSG). Wind systems with DFIG are introduced in [6–7]. One main problem associated is that the existing of the gearbox links the wind turbine to the generator, which increases system maintenance expenses and mechanical faults suffering. Wind systems with PMSG are introduced in [8–16]. With which a smaller pole pitch can be used, the generator can rotate at lower velocity at the rate of 20–200 r/min while providing induced voltage high enough, eliminating the use of gearbox. In [8–13], fully controlled PWM converter is used to couple the generator to utility grid. The vector control PWM was adopted by generator-side converter (rectifier) and grid-side converter (inverter), achieving MPPT and decoupling control of active and reactive power injected into the grid. Thus, two sets of fully controlled bridge are needed, which increase the cost and instability of the system. In [14–16], a new structure eliminateing one controlled converter is adopted, in which a diode rectifier and DC boost chopper circuit take place of the controlled rectifier. However, they can only be adopted in small wind systems due to the capacity of boost circuit. In this paper, a novel wind energy conversion system based on hybrid excitation synchronous machine (HESM) is proposed. The whole system topology is shown in Fig.1.

Received Mar.23, 2010; Revised Oct.3, 2010
Project supported by Delta Power Electronic Science and Education Development (Grant No.DRES2007002)
Corresponding author RUAN Yi, Ph D, Prof, E-mail: yraun@mail.shu.edu.cn

The back electromotive force of the generator is firstly converted into DC voltage with a diode, then a fully controlled voltage source inverter (VSI) is used to feed the power into the utility grid. The DC link voltage is adjusted to a reference voltage by a PI regulator, and the inverter currents are controlled synchronously to be inphase with utility grid. The excitation current of HESM is provided through a DC buck circuit.

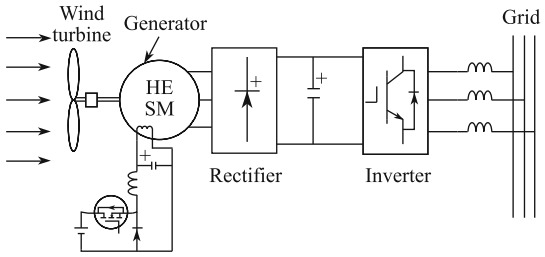

Fig.1 Topology of system

The following part of this paper is organized as follows. In Section 1, the mathematical model of HESM and its excitation current control are introduced. In Section 2, the model of three phase grid connected inverters and its control strategy are discussed. In Section 3, the MPPT method is explained based on the aerodynamic principle of wind turbine. In Section 4, experimental results are presented, and the conclusion of the overall system is made in Section 5.

1 Generator control

1.1 Mathematical model of HESM

The structure of HESM used in this paper is shown in Fig.2[17] which allows one to control the excitation current of the generator without brushes. Contrasted with the traditional permanent magnet synchronous machine (PMSM), the principles of the hybrid excitation are based on two flux sources: permanent magnets and excitation coil, which is not included in PMSM. A DC stator coils (avoiding sliding contacts) produce a rotating field

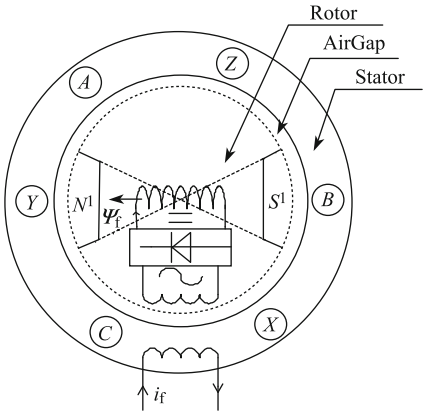

Fig.2 Structure of HESM

which is equivalent to the one produced by the rotor excitation coils in classical wound excitation synchronous machine through a diode rectifier in the rotor.

This structure brings in a single degree of freedom in terms of mathematical model complexity. However, in the electromagnetic aspect, only an adjustable excitation coil is added to the rotor. Then the HESM model in the synchronous rotational coordinate (dq0 coordinate) can be built to eliminate the nonlinear relation which exists in the differential equation in the original coordinate. The HESM can be described by the following relations between currents and fluxes:

$$\begin{aligned}\psi_{\mathrm{d}} &= L_{\mathrm{d}} i_{\mathrm{d}} + M_{\mathrm{sf}} i_{\mathrm{f}} + \psi_{\mathrm{pm}},\\ \psi_{\mathrm{q}} &= L_{\mathrm{q}} i_{\mathrm{q}},\\ \psi_{\mathrm{f}} &= \frac{3}{2} M_{\mathrm{sf}} i_{\mathrm{d}} + L_{\mathrm{f}} i_{\mathrm{f}},\end{aligned} \tag{1}$$

where L_{d}, L_{q} are the d and q axis inductance, M_{sf} mutual-inductance coupling the excitation winding and the armature winding, L_{f} self-inductance of the excitation winding. ψ_{pm}, ψ_{f}, ψ_{d}, ψ_{q}, are the flux of the permanent magnet, excitation winding, d axis, q axis, respectively. i_{d}, i_{q}, i_{f} are the direct current, quadrature current, and excitation current of the generator respectively.

The expressions of voltages are given as

$$\begin{aligned}\frac{\mathrm{d}i_{\mathrm{q}}}{\mathrm{d}t} &= \frac{u_{\mathrm{q}} - R_1 i_{\mathrm{q}} - \omega(L_d i_{\mathrm{d}} + M_{\mathrm{sf}} i_{\mathrm{f}} + \psi_{\mathrm{pm}})}{L_{\mathrm{q}}},\\ \frac{\mathrm{d}i_{\mathrm{d}}}{\mathrm{d}t} &= \frac{L_{\mathrm{f}}(u_{\mathrm{d}} + \omega L_{\mathrm{q}} i_{\mathrm{q}} - R_1 i_{\mathrm{d}}) - M_{\mathrm{sf}}(u_{\mathrm{f}} - R_{\mathrm{f}} i_{\mathrm{f}})}{L_{\mathrm{f}} L_{\mathrm{d}} - 1.5 M_{\mathrm{sf}}^2},\\ \frac{\mathrm{d}i_{\mathrm{f}}}{\mathrm{d}t} &= \frac{L_{\mathrm{d}}(u_{\mathrm{f}} - R_{\mathrm{f}} i_{\mathrm{f}}) - 1.5 M_{\mathrm{sf}} L_{\mathrm{f}}(u_{\mathrm{d}} + \omega L_{\mathrm{q}} i_{\mathrm{q}} - R_1 i_{\mathrm{d}})}{L_{\mathrm{f}} L_{\mathrm{d}} - 1.5 M_{\mathrm{sf}}^2}.\end{aligned} \tag{2}$$

The torque of the generator can be described as

$$T_{\mathrm{e}} = \frac{3}{2} p_{\mathrm{r}}(i_{\mathrm{q}} \psi_{\mathrm{pm}} + i_{\mathrm{d}} i_{\mathrm{q}}(L_{\mathrm{d}} - L_{\mathrm{q}}) + M_{\mathrm{sf}} i_{\mathrm{f}}(i_{\mathrm{q}} - i_{\mathrm{d}})), \tag{3}$$

where p_{r} is the number of pole pairs.

1.2 Control strategy for excitation current

A current closed-loop buck circuit is designed to control the excitation current of the HESM, as shown in Fig.3.

In order to get a stable DC link voltage, a stable rotor flux is needed for the generator. Then current ripples which exist in traditional buck circuit must be reduced. An LC filter is added to the circuit for harmonic reduction, and with the PI regulator, a constant excitation current followed a given current can be obtained. Hence a stable magnetic field can be achieved.

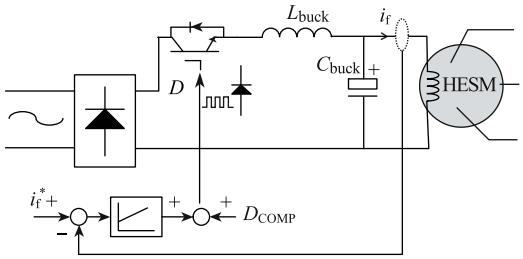

Fig.3 Topology of buck circuit

2 Grid side inverter control

2.1 Mathematical model

Three phase grid-connected inverter is a key component which connects the generator system to the grid. Its performance has a great effect on the whole system[18−21]. Grid vector oriented control strategy is widely used in the three phase VSI. The topology of VSI adopted in this paper is shown in Fig.4.

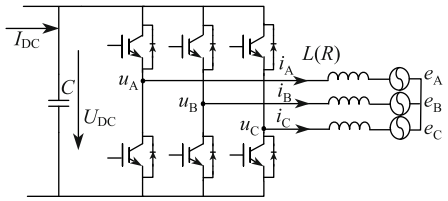

Fig.4 Three phase grid connected VSI

i_A, i_B, i_C are the output currents of the inverters, and the reference direction is shown in the Fig.4. u_A, u_B, u_C are the output voltages of the inverter, and e_A, e_B, e_C are the three phase grid voltages. U_{dc} is the DC bus voltage, and $L(R)$ is the grid side filter inductor and its resistance between the grid and the inverter.

The three phase grid voltages are defined as follows:

$$\begin{aligned} e_A &= E\cos(\omega_1 t),\\ e_B &= E\cos\left(\omega_1 t - 2\frac{\pi}{3}\right),\\ e_C &= E\cos\left(\omega_1 t + 2\frac{\pi}{3}\right), \end{aligned} \tag{4}$$

where E is the maximum phase amplitude of grid voltage, and ω_1 is the synchronous angular frequency of the grid.

In the $d-q$ coordinator, the voltage synthesized vector is fixed at d axis. Then the d axis component of resultant vector of grid voltage e_s becomes e_d, and q axis component becomes zero. The dynamic model of the grid connected VSI is described as

$$\begin{aligned} L\frac{\mathrm{d}i_\mathrm{d}}{\mathrm{d}t} &= e_\mathrm{d} - S_\mathrm{d}U_\mathrm{dc} - Ri_\mathrm{d} + L\omega i_\mathrm{q},\\ L\frac{\mathrm{d}i_\mathrm{q}}{\mathrm{d}t} &= -S_\mathrm{q}U_\mathrm{dc} - Ri_\mathrm{q} - L\omega i_\mathrm{d},\\ C\frac{\mathrm{d}U_\mathrm{dc}}{\mathrm{d}t} &= -\frac{3}{2}S_\mathrm{d}i_\mathrm{d} - \frac{3}{2}S_\mathrm{q}i_\mathrm{q} + I_\mathrm{dc}, \end{aligned} \tag{5}$$

where s_d, s_q are the switch function in the $d-q$ rotating reference axes respectively, and i_d, i_q are the output current of the inverter in the $d-q$ rotating reference axes respectively. All of them are shown in $d-q$ rotating coordinator.

The output power is given as

$$\begin{aligned} P &= \frac{3}{2}e_\mathrm{d}i_\mathrm{d},\\ Q &= \frac{3}{2}e_\mathrm{d}i_\mathrm{q}. \end{aligned} \tag{6}$$

2.2 Control strategy for the grid side inverter

The control block diagram of the grid side inverter is shown in Fig.5. From (6), it can be obtained that the active and reactive power are proportionate to direct and quadrature current respectively, while the d and q current can be controlled separately according to (5), though coupling item which is derived from (4) can still be found between the active and reactive power control loop. The d-axis control channel includes two control loops, the outer DC voltage control loop and the inner active current control loop. The DC reference voltage is set to a constant according to the basic request of

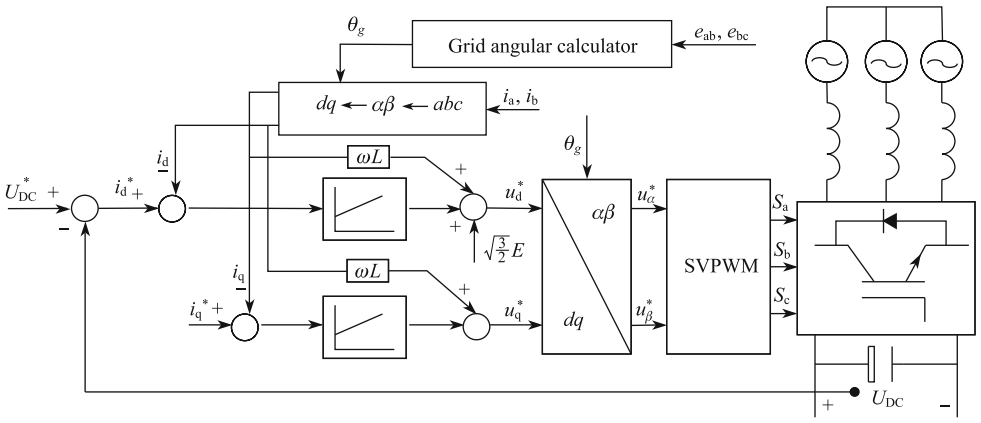

Fig.5 Block diagram of grid side inverter controller

system, and the active current reference is set to the output of outer DC voltage loop, which assures all the active power coming from the generator is coupling to the utility grid instantaneously. The q-axis control channel includes one control loop, the reactive current control loop. The reference of q-axis current is set to a value according to the inactive power compensation request and the capability of the system.

3 MPPT control

3.1 Characteristic wind turbine

The torque produced by a wind turbine is given by

$$P_{\mathrm{T}} = 0.5\rho R^2 c_{\mathrm{p}} \nu^3, \tag{7}$$

where R is the radius of turbine, v the wind velocity, ρ the air density. c_{p} is the utilization coefficient of wind power, and it is a function of the blade pitch angle ∂ and tip speed ratio λ. ∂ is usually fixed for a regular running wind power generation system. Then the magnitude of c_{p} is decided as

$$\lambda = \frac{R\omega}{\nu}, \tag{8}$$

where ω is the turbine angular velocity.

The typical $c_{\mathrm{p}} - \lambda$ curve of a certain wind speed is shown in Fig.6. The output power characteristic turbine at different angular velocity and different wind velocity is shown in Fig.7.

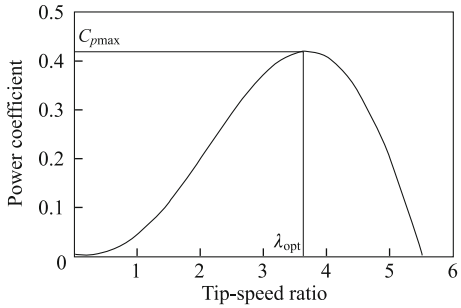

Fig.6 $c_p - \lambda$ characteristics

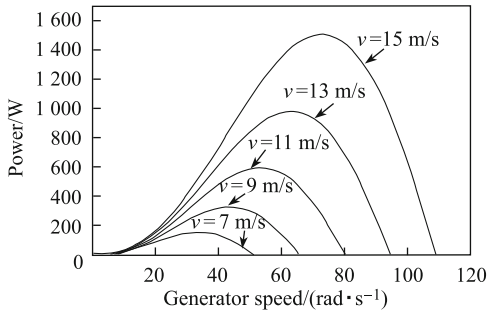

Fig.7 Turbine output power-generator speed characteristics

From Figs.5 and 6, it can be seen that the power coefficient is maximum at a certain value of tip speed ratio called optimum tip speed ratio λ_{opt}, and the turbine should always operate at λ_{opt}. In order to capature the maximum possible energy, it is possible to rotate at the optimum speed by controlling the rotational speed of the turbine.

3.2 Control strategy for MPPT

The MPPT controller is shown in Fig.8. It executes as follows: First, an optimal generator speed is obtained by means of calculating the transient output power of the inverter. Then, with the feedback of real generator speed, a given HESM excitation current is obtained by a PI regulator. Figure 9 shows the flowchart of MPPT logic.

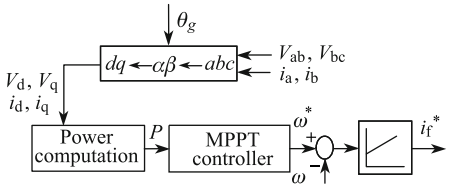

Fig.8 Control scheme of MPPT control

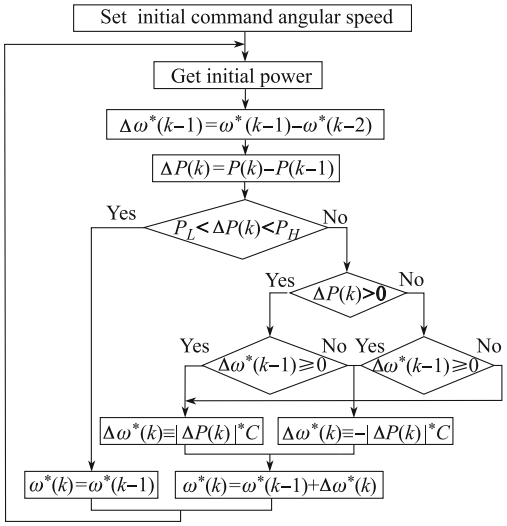

Fig.9 Flow chart of MPPT controller

The active power $P_{\mathrm{o}}(k)$ is measured. If the difference between its values at present and previous sampling instants $\Delta P_{\mathrm{o}}(k)$ is within a specified lower and upper power limits PL and PM respectively, no action is taken. However, if the difference is outside this range, the certain control action is taken. The control action taken depends upon the magnitude and direction of change in active power, due to the change in command speed.

If the changing of the magnitude in the command speed in a control cycle is decided by the product of magnitude of power error of $P(k)$ and C, whose values are determined by the speed of the wind, and C is

a constant. During the maximum power point tracking control process, this product decreases slowly and finally equal to 0 at the peak power point.

4 Experiment verification

A DC motor with particular torque control is used to emulate the wind turbine in the experiment. In the prototype, a 3 kW motor is used, the program implement by means of reading the input data like wind velocity, turbine angular velocity, and calculating the corresponding coefficient curve. Then the power of wind turbine at the moment can be calculated, so the given torque of motor. The imitation scheme of wind turbine is shown in Fig.10.

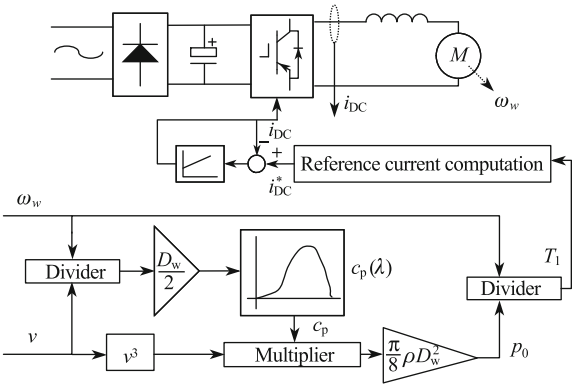

Fig.10 Emulation scheme of the wind turbine

The parameters of the HESM used in the experiment are shown in Table 1.

Table 1 Parameters of the HESM

Parameter	Value	Parameter	Value
P_N/kW	10	L_d(H)	0.026 7
P_{max}/kW	15	L_q(H)	0.030 3
Ra/Ω	0.459	M_{af}	0.412 8
Rf/Ω	143.4	ψ_{pm}	1.196 5

Figure 11 shows the characteristic waveforms of the wind velocity and the corresponding generator angular velocity. The generator speed varies from 750 to 1 050 r/min when the speed of wind rises from 7.5 m/s to 10.5 m/s. Then as the wind speed follows to 8.5 m/s, the generator speed drops to 850 r/min, and the system always runs at the point tracked to maximum power.

Figure 12 shows the fluctuation of DC link voltage as the wind speed varies is smaller than 20 V. A phase voltage and current of the inverters is shown in Fig.13 when the d axis current is set to 0 for a unity power factor condition.

In Fig.14, d axis current is set to a 5 value for reactive compensation, waveforms of voltage and current has a certain phase difference. All of them show a good

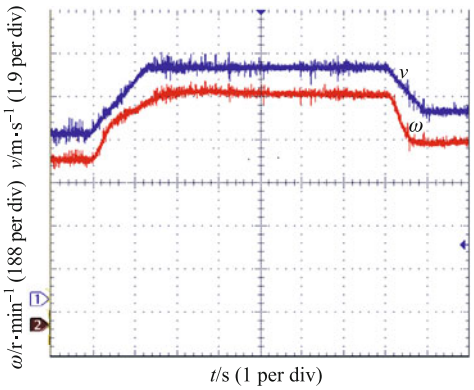

Fig.11 Characteristic waveforms of the wind speed and the corresponding generator speed

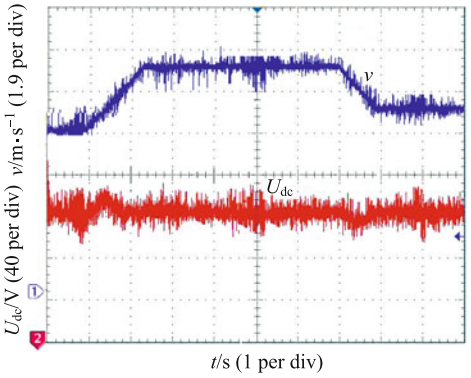

Fig.12 Fluctuation of DC link voltage

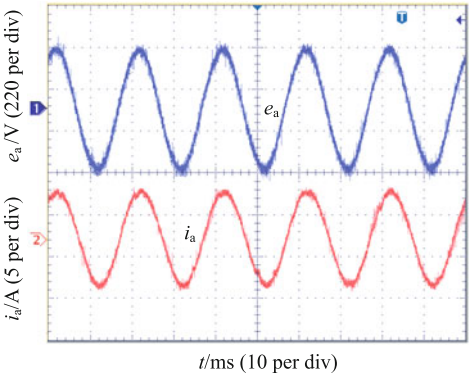

Fig.13 Waveforms of the inverter voltage and current in unit power factor

performance of the whole system.

5 Conclusions

This paper proposed a direct-drive type wind power generation system based on HESM. The MPPT control strategy corresponding to the structure of the system was given, and the decoupling control of active and inactive power based on the mathematical model of the whole system was proposed. Be contrast to the conventional direct-driven types, the whole system and control method is very simple. Experimental results show that

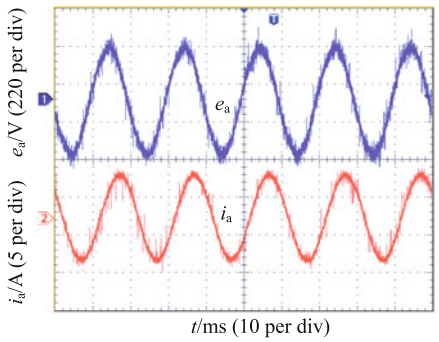

Fig.14 Waveforms of the inverter voltage and current with reactive compensation

an excellent real-time performance of the MPPT method and a good current waveform of the whole system.

References

[1] Carrasco J M, Franquelo L G, Bialasiewicz J T, Galvan E, Portillo-Guisado R C, Prats M A M, Leon J I, Moreno-Alfonso N. Power-electronic systems for the grid integration of renewable energy sources: A survey [J]. IEEE Transactions on Industrial Electronics, 2006, 53(4): 1002–1016.

[2] Heier S. Grid integration of wind energy conversion systems [M]. Hobo-ken: Wiley, 1998.

[3] Boukhezzar B, Siguerdidjane H. Nonlinear control of variable speed wind turbines without wind speed measurement [C]// Proceedings of 44th Conference on Decision and Control, and the European Control Conference, Serville, Spain. 2005: 3456–3461.

[4] Koutroulis E, Kalaitzakis K. Design of a maximum power tracking system for wind-energy-conversion applications [J]. IEEE Transactions on Industrial Electronics, 2006, 53(2): 486–494.

[5] Li C H, Zhu X J, Sui S, Hu W Q. Maximum power point tracking of a photovoltaic energy system using neural fuzzy techniques [J]. Journal of Shanghai University (English Edition), 2009, 13(1): 29–36.

[6] Tapia A, Tapia G, Ostolaza J X, Saenz J R. Modeling and control of a wind turbine driven doubly fed induction generator [J]. IEEE Transactions on Energy Conversion, 2003, 18(2): 194–204.

[7] Qiao W, Zhou W, Aller J M, Harley R G. Wind speed estimation based sensorless output maximization control for a wind turbine driving a DFIG [J]. IEEE Transactions on Industrial Electronics, 2008, 23(3): 1156–1169.

[8] Higuchi Y, Yamamura N, Ishida M, Hori T. An improvement of performance for small-scaled wind power generating system with permanent magnet type synchronous generator [C]// IEEE Industrial Electronics Society Conference, Nagoya, Japan. 2000, 2: 1037–1043.

[9] Senjyu T, Tamaki S, Muhando E, Urasaki N, Kinjo H, Funabashi T, Fujita H, Sekine H. Wind velocity and rotor position sensorless maximum power point tracking control for wind generation system [J]. Renewable Energy, 2006, 31(11): 1764–1775.

[10] Chinchilla M, Arnaltes S, Burgos J C. Control of permanent magnet generators applied to variable-speed wind-energy systems connected to the grid [J]. IEEE Transactions on Energy Conversion, 2006, 21(1): 130–135.

[11] Li S H, Haskew T A. Characteristic study of vector-controlled direct driven permanent magnet synchronous generator in wind power generation [C]// Power Engineering Society General Meeting—Conversion and Delivery of Electrial Energy in the 21st Century, Pittsburgh, USA. 2008, DOI: 10.1109/PES.2008.4596191.

[12] Srighakollapu N, Sensarma P S. Sensorless maximum power point tracking control in wind energy generation using permanent magnet synchronous generator [C]// Industrial Electronics 34th Annual Conference of IEEE, Orlando, USA. 2008: 2225–2230.

[13] Esmaili R, Xu L, Nichols D K. A new control method of permanent magnet generator for maximum power tracking in wind turbine application [C]// IEEE Power Engineering Society General Meeting, San Francisco, California, USA. 2005, 3: 2090–2095.

[14] Amei K, Takayasu Y, Ohji T, Sakui M. A maximum power control of wind generator system using a permanent magnet synchronous generator and a boost chopper circuit [C]// Proceedings of the Power Conversion Conference, Osaka, Japan. 2002, 3: 1447–1452.

[15] Song S, Kang S, Hahm N. Implementation and control of grid connected AC-DC-AC power converter for variable speed wind energy conversion system [C]// IEEE Applied Power Electronics Conference and Exposition, Florida, USA. 2003: 154–158.

[16] Chen Y G, Wang Z Q. A control strategy of direct driven permanent magnet synchronous generator for maximum power point tracking in wind turbine application [C]// International Conference on Electrical Machines and Systems, Wuhan, China. 2008: 3921–3926.

[17] Zhang H J, Tang R Y. Theory and design of hybrid excitation permanent magnet synchronous generators [C]// International Conference on Electrical Machines and System, Shenyang, China. 2001, 2: 898–900.

[18] Wu R, Dewan S B, Slemon G R. Analysis of an AC-to-DC voltage source converter using PWM with phase and amplitude control [J]. IEEE Transactions on Power Electronics, 1991, 27(2): 355–364.

[19] Noguchi T, Tomiki H, Kondo S, Takahashi I. Direct power control of PWM converter without power-source voltage sensors [J]. IEEE Transactions on Industrial Application, 1998, 34(3): 473–479.

[20] Malinowski M, Jasinski M, Kazmierkowski M P. Simple direct power control of three-phase PWM rectifier using space-vector modulation (DPC-SVM) [J]. IEEE Transactions on Industrial Electronics, 2004, 51(2): 447–454.

[21] Kazmierkowski M P, Malesani L. Current control techniques for three-phase voltage-source PWM converters: A survey [J]. IEEE Transactions on Industrial Electronics, 1998, 45(5): 691–703.

(Editor HONG Ou)